# Mechanism of hydrogen formation during the corrosion of Mg17Al12

Serge Al Bacha, Arnaud Desmedt, Mirvat Zakhour, Michel Nakhl, Jean-Louis Bobet

Electrochemistry Communications 119 (2020) 106813

Contents lists available at ScienceDirect

Electrochemistry Communications

journal homepage: www.elsevier.com/locate/elecom

# Mechanism of hydrogen formation during the corrosion of $Mg_{17}Al_{12}$

S. Al Bacha[a,b,*], A. Desmedt[c], M. Zakhour[a], M. Nakhl[a], J.-L. Bobet[b]

[a] LCPM/PR2N, Lebanese University, 90656 Jdeidet El Metn, Lebanon
[b] ICMCB – CNRS, University of Bordeaux, UPR 9048, F-33600 Pessac, France
[c] ISM – CNRS, University of Bordeaux, UMR 5255, F-33405 Talence, France

ARTICLE INFO

*Keywords:*
Hydrogen
Monovalent Mg
Corrosion
$Mg_{17}Al_{12}$
Raman
$Mg^+/MgH^+$

ABSTRACT

Previous investigations (DFT calculations) showed that hydrogen atoms adsorption and $H_2$ desorption can occur on MgO and $Al_2O_3$ and that H atoms can diffuse on Mg and Al surfaces. However, these three simultaneous actions, *i.e.* H adsorption, H diffusion and $H_2$ desorption, have not been experimentally proved. In this paper, we propose a mechanism of formation of $H_2$ during the corrosion of an intermetallic compound $Mg_{17}Al_{12}$ in 3.5 wt. % NaCl aqueous solution based on *in situ* Raman spectroscopy analysis. We found that, through the passivation zone (*e.g. E* varying from the open circuit potential (OCP) to +100 mV/OCP), the oxide layer is destroyed in favor of the appearance of Mg and H atoms. Moreover, the formed H atoms are adsorbed on the oxide surface and then diffuse on either the oxide surface or the unreacted metal surface where they recombine forming $H_2$. *In situ* Raman measurements during anodic polarization experimentally prove, for the first time, the formation of a reaction intermediate which weakens the H–H bond. The obtained results explain the mechanism of hydrogen production under anodic polarization of the intermetallic compound at normal conditions of temperature and pressure.

## 1. Introduction

The spillover effect is generally defined as the transport of an active species (*e.g.* $H_2$) adsorbed or formed on a surface to another surface that does not adsorb or form the active species under the same conditions [1]. Reverse spillover of hydrogen is explained as the migration of adsorbed H atoms from a receptor to a source, where they recombine and desorb as $H_2$ molecules [2]. The interaction of a hydrogen atom/hydrogen molecule and of hydrogen containing molecules with MgO [3–11] and $Al_2O_3$ [12,13] has been studied both experimentally and theoretically. The evidence of heterolytic splitting of $H_2$ was reported a long time ago by experiments performed on MgO powders [5,10] and by *ab initio* calculations [9,11,14,15]. An unpaired hydrogen (*i.e.* H atom) can diffuse on O-sites of MgO above the surface with lower activation energy than that of paired hydrogens, where the diffusion distorts the surface [16]. The interaction between a hydrogen atom and the surface of MgO is weak as the binding energy of a hydrogen atom is small for MgO and the change in free enthalpy is strongly positive when H atoms migrate to the surface of a nonreducible support [3]. $H_2$ molecules dissociate at (1 0 0) MgO surface defects [17], because defects have a radical character and can thus bond (radical) H atoms [18]. The reconstructed MgO (1 1 1) surface exposes neighboring low-coordination $Mg^{2+}$ and $O^{2-}$ ions that bond hydrogen to form $OH^-$ and $MgH^+$ [19]. Similarly, hydrogen atoms adsorb dissociatively on aluminum and its oxide with the formation of Al-H [20] and $H^-$ [13] respectively. Additionally, the diffusion of atomic H on the Mg surface and Al surface is energetically favorable [20,21].

Magnesium alloys are promising lightweight materials for aerospace, automobile, consumer electronics and biodegradable implants due to their low density and high specific strength [22–25]. Mg-Al alloys are the most common category of magnesium alloys where Mg can form with Al an intermetallic compound $Mg_{17}Al_{12}$. Nevertheless, magnesium alloys are reactive in marine environments [26–28]. The corrosion behavior of pure $Mg_{17}Al_{12}$ has been reported previously [29,30]. The hydrogen produced during the corrosion of Mg-based materials can be used as an energy carrier for clean energy economy.

Here, we report the examination of the surface modification by collecting vibrational Raman spectra during anodic polarization of $Mg_{17}Al_{12}$ in 3.5 wt.% NaCl solution. Increasing the potential beyond the OCP led us to observe the hydrogen formation, by the cathodic reaction (*i.e.* reduction of water), and its possible adsorption on the formed MgO and $Al_2O_3$ during the corrosion of $Mg_{17}Al_{12}$. Diffusion of H atoms from the oxide to the metal surface is verified experimentally by the integration of peaks from the corroded surface in the Raman spectra.

* Corresponding author at: LCPM/PR2N, Lebanese University, 90656 Jdeidet El Metn, Lebanon and ICMCB, University of Bordeaux, 87 av. Dr. Schweitzer, 33600 Pessac, France.
*E-mail address:* serge.al-bacha@icmcb.cnrs.fr (S. Al Bacha).

https://doi.org/10.1016/j.elecom.2020.106813
Received 28 July 2020; Received in revised form 13 August 2020; Accepted 13 August 2020
Available online 19 August 2020

## 2. Material and methods

Before corrosion tests, the as-cast $Mg_{17}Al_{12}$ (Extended Data Fig. 1) was mechanically polished up to 4000 grit SiC paper with absolute ethanol as lubricant until a clean surface was obtained. A conventional three-electrode configuration was used with $Mg_{17}Al_{12}$ as the working electrode, a saturated calomel electrode (SCE) as the reference electrode, and a titanium grid as the counter electrode in a model seawater solution (*i.e.* 3.5 wt.% NaCl aqueous solution) to perform the "electrochemical measurement" using a Biologic SP-150 potentiostat with a current resolution of 760 pA and a voltage resolution of 5 μV. For the anodic polarization test, the sample was maintained for 60 min at OCP in the model seawater solution until it reaches its steady-state as previously observed [29], then, the potential was switched to −50 mV/OCP and scanned up to 100 mV/OCP at 0.05 mV/s. Therefore, $Mg_{17}Al_{12}$ was immersed in the solution for 110 min: 60 min for the OCP measurement and 50 min for the anodic polarization test. During the anodic polarization (from −50 mV/OCP to +100 mV/OCP at 0.05 mV/s), vibrational Raman spectra were recorded with a Labram HR Evolution Spectrometer (Horiba Jobin Yvon, Villeneuve d'Ascq, France) using a 532 nm wavelength laser as the excitation source. An Olympus LUMPlanFl 100×/1.00 water immersion objective allows the incident laser beam to be focused on a micrometer-sized part of the sample (Extended Data Fig. 2a and b). Raman spectra were collected in the 400–4380 $cm^{-1}$ range near a corroded area (Extended Data Fig. 2c). Reference spectra acquired by measuring the Raman spectra of the salt solution (*e.g.* 3.5 wt.% NaCl), Mg, Al (pure Al (fcc crystal structure) do not show Raman spectra in similarity to zirconium metal (bcc crystal structure) [31] so that the peaks observed in Extended Data Fig. 3c are attributed to the thin oxide layer covering Al particles), MgO and Mg $(OH)_2$ were taken as reference (Extended Data Fig. 3). The corroded surface of $Mg_{17}Al_{12}$ after anodic polarization was analyzed using a TESCAN VEGA3 SB scanning electron microscope equipped with an energy dispersive X-ray spectrometer for the identification of magnesium, aluminum and oxygen.

## 3. Results and discussion

### 3.1. Surface modification during anodic polarization

Fig. 1a shows the evolution of peaks in the Raman spectra for different duration of the polarization test (where 60 min is the start of the polarization test).

Peaks attributed to pure Mg crystalline modes (between 960 $cm^{-1}$ and 1000 $cm^{-1}$), Mg–O vibration (between 1030 $cm^{-1}$ and 1170 $cm^{-1}$), Mg–OH vibration (between 3600 $cm^{-1}$ and 3700 $cm^{-1}$) were observed as well as other peaks during the anodic polarization of $Mg_{17}Al_{12}$. The peaks shown in the 400–2000 $cm^{-1}$ (Extended Data Fig. 4a) are identified as follows: 500–630 $cm^{-1}$ is characteristic of Mg materials (in pure Mg, $Mg_{17}Al_{12}$ or MgO), 630–720 $cm^{-1}$ to NaCl, MgO and $Mg_{17}Al_{12}$, between 960 $cm^{-1}$ and 1000 $cm^{-1}$ to pure Mg crystalline modes, between 1030 $cm^{-1}$ and 1170 $cm^{-1}$ to MgO, the broad peaks in the 1230–1500 $cm^{-1}$ and 1500–1720 $cm^{-1}$ range may be respectively (i) an overlap of the fluorescence of $Mg(OH)_2$ and the OH bending of water and (ii) $Al_2O_3$ present on the surface of Al. Furthermore, the broad peak in the 3000–3770 $cm^{-1}$ range (Extended Data Fig. 4b) consists of three overlapped peaks: those of the OH stretching modes centered at 3233 $cm^{-1}$ and 3393 $cm^{-1}$ and the third peak at 3650 $cm^{-1}$ is attributed to Mg-OH vibration (Extended Data Fig. 3d and e). The two peaks (denoted H1 and H2 respectively) shown in the 4015–4135 $cm^{-1}$ range and 4135–4255 $cm^{-1}$ range are not, we believe, identified as $H_2$; the vibration of dissolved $H_2$ in water is located at 4138 $cm^{-1}$ [32]. Meanwhile H1 and H2 are observed in the vibrational region of molecular hydrogen. These two peaks could be attributed to the molecular hydrogen formed at the interface solid/electrolyte. The broad H2 peak is characteristic of highly bonded molecular hydrogen interacting with its environment, and exhibits a frequency slightly higher than that of dissolved $H_2$ in water. The low vibration frequency of H1 indicates a weaker intramolecular interaction compared to the standard H–H interaction. This weaker interaction may be a result of reinforced interactions between the formed hydrogen and its environment. On one hand, Song *et al.* [33] considered that monovalent magnesium ion ($Mg^+$) is formed during the corrosion of magnesium. On the other hand, the formation of $MgH^+$ [19] in MgO was reported previously. These species may weaken the H–H bond, favoring the appearance of a shifted Raman peak H1. Even though Ma *et al.* [34] provided an estimation of the free energy of formation of $Mg^+$ implying that it may be the expected surface species, this hypothesis cannot be adopted without evaluating the effect of $Mg^+$ on the vibration frequency of the H–H bond.

Fig. 1b shows the variation of the peaks attributed to Mg, MgO, Mg $(OH)_2$ and H1 as a function of the applied potential. Applying a higher potential than the OCP leads to the destruction of the passivation layer (MgO), localized by pitting corrosion induced by $Cl^-$ ions [35], favoring the appearance of fresh Mg and Mg-OH. Furthermore, the intensity of H1 peak increases simultaneously with both the Mg and Mg-OH peaks. The proposed mechanism of $H_2$ generation after the breaking of the passivation layer is illustrated in Fig. 2.

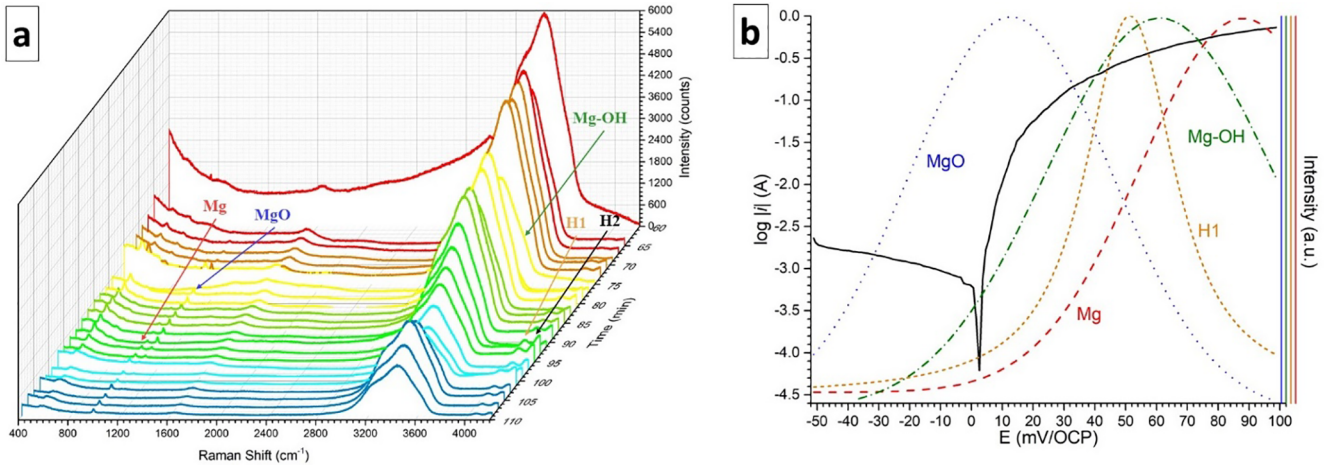


**Fig. 1.** a) Vibrational Raman spectra of $Mg_{17}Al_{12}$ under anodic polarization as a function of time and b) anodic polarization plot of $Mg_{17}Al_{12}$ from −50 mV/OCP to + 100 mV/OCP and the corresponding variation of the instensities of the Mg peak (960–1000 $cm^{-1}$), MgO peak (1030–1110 $cm^{-1}$), Mg-OH peak (3650 $cm^{-1}$), and H1 peak (4015–4135 $cm^{-1}$).

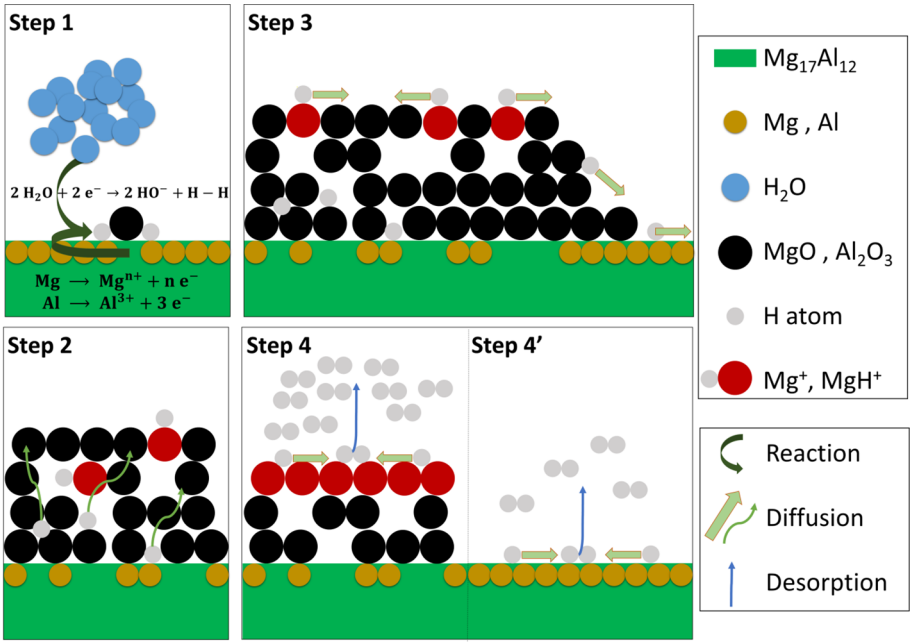


**Fig. 2.** Scheme of hydrogen production during $Mg_{17}Al_{12}$ anodic polarization considering the generation, the adsorption and the diffusion of H atoms as well as $H_2$ desorption.

The author's previous work shows that the reaction of $Mg_{17}Al_{12}$ in HCl produced $Mg(OH)_2$, $Al(OH)_3$ and unreacted Al [36]. Reaction of $Mg_{17}Al_{12}$ with water generates H atoms by the reduction of $H_2O$ (step 1) and forms MgO and $Al_2O_3$ on the surface (Extended Data Fig. 5). The formed H atom diffuses through the metal oxide film and is adsorbed on MgO and $Al_2O_3$ to form $MgH^+$ [19] or to interact with $H_2$ (step 2). Since the diffusion of H on Mg and Al is favorable [18,19] (step 3), two H atoms recombine either on the MgO-$Al_2O_3$ surface (step 4) or the unreacted $Mg_{17}Al_{12}$ surface (step 4′) to form an $H_2$ molecule and desorb. However, since the H-atoms are formed during the corrosion of Mg, step 4 is more favorable than step 4′.

### 3.2. Corroded zone mapping

Raman mapping of the corroded surface after the anodic polarization test (Fig. 3 and Extended Data Fig. 6) revealed the presence of more peaks than those shown in Fig. 1.

After the reaction of $Mg_{17}Al_{12}$ with salt water, the corroded surface is covered by Mg and MgO (Fig. 3b, c and d), while energy dispersive X-ray (EDX) mapping (Extended Data Fig. 5) revealed the presence of two zones: the corroded surface (consisting of Mg-Al-O) and the non-corroded surface (consisting of Mg-Al). H1 and H2 enrichment is found on the oxide surface (Fig. 3e and f) proving the adsorption of H atoms on MgO and $Al_2O_3$, while the intensity of H1 decreases in the direction of the Mg-Al surface. The formation of the hydrogen atoms is dependent on the formation of the oxide layer – H atoms are formed during the corrosion of $Mg_{17}Al_{12}$. Subsequently, H atoms formed during the corrosion of $Mg_{17}Al_{12}$ adsorb on the metal oxide surface and diffuse either on the oxide surface or on the metal surface. In fact, H diffusion is favorable on both the oxide and the intermetallic surface [16,20,21]. Since H atoms are formed in the corroded zone (MgO and $Al_2O_3$), the interaction of two H atoms on this surface is more probable than that on the non-corroded surface due to the smaller diffusion path. As a consequence, $H_2$ recombination and desorption is detected over the oxide surface. The variation of the other observed peaks is presented in Extended Data Fig. 6.

Huang *et al.* [37] stated that "Mg is first electrochemically oxidized to the intermediate active univalent $Mg^+$ ion on the Mg surface only in the film-free areas". Nevertheless, Fig. 3e shows that the highest intensity of H1 peak is in the film area (corroded surface) implying that $Mg^+$ and/or $MgH^+$ is formed in this zone. Moreover, it is supposed that the univalent $Mg^+$ reacts immediately with water converting into $Mg^{2+}$ and producing hydrogen [37]. If this is true, H1 peak, attributed to the weakening of the H–H bond by $Mg^+$ [33,34] and/or $MgH^+$ [19], should not be detectable. In fact, this peak persists after the anodic polarization implying that $Mg^+$ and/or $MgH^+$ are chemically stable and does not immediately oxidize into $Mg^{2+}$.

## 4. Conclusion

In summary, our work clearly highlights the mechanism of $H_2$ production during the anodic polarization of $Mg_{17}Al_{12}$ in model seawater solution (*i.e.* 3.5 wt.% NaCl).

- A mechanism of formation of $H_2$ during the corrosion of $Mg_{17}Al_{12}$ was proposed:
- H atoms formed on $Mg_{17}Al_{12}$ are adsorbed at the surface (Raman peak H2);
- H atoms then diffuse in the formed oxide layer and on the intermetallic surface.
- A reaction intermediate ($Mg^+$ and/or $MgH^+$) is formed during the anodic polarization and weakens the standard H–H bond (Raman peak H1).
- The interaction of two H atoms on the oxide surface (more probable) or on the uncorroded surface (less probable) lead to the recombination and desorption of molecular $H_2$.
- The mechanism of hydrogen production (*i.e.* H atoms generation, adsorption, diffusion, recombination and $H_2$ desorption) is experimentally proven by vibrational Raman spectroscopy.

Looking forward, we anticipate that our experimental results will also prove valuable when exploring the effect of monovalent Mg ion in the corrosion mechanism of metals and their alloys.

## CRediT authorship contribution statement

**S. Al Bacha:** Methodology, Formal analysis, Investigation, Writing - original draft, Visualization. **A. Desmedt:** Validation, Investigation,

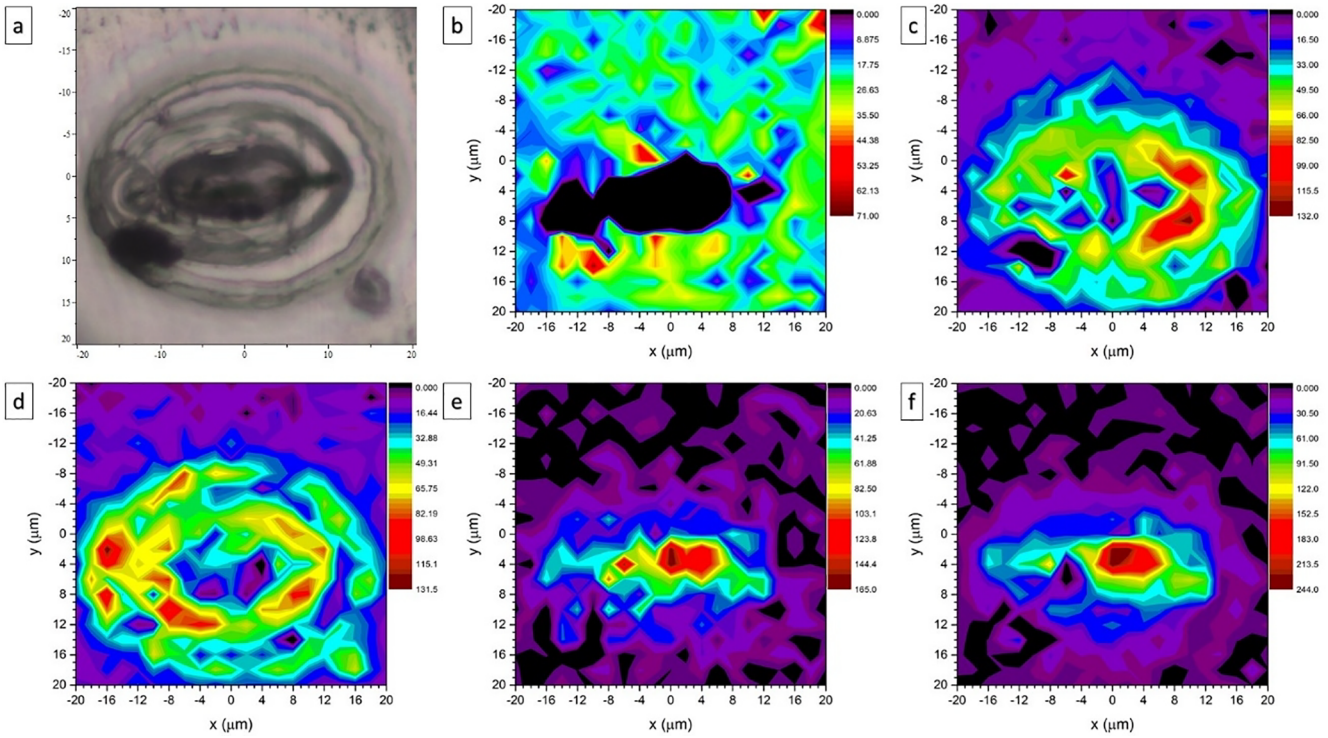


**Fig. 3.** a) Optical micrograph of the scanned area test and the variation of the intensity of the following peaks: b) $Mg_{17}Al_{12}$ (700–900 $cm^{-1}$), c) Mg (960–1000 $cm^{-1}$), d) MgO (1030–1110 $cm^{-1}$), e) H1 (4015–4135 $cm^{-1}$), and f) H2 (4135–4255 $cm^{-1}$).

Resources, Supervision. **M. Zakhour:** Validation, Project administration, Supervision. **M. Nakhl:** Validation, Project administration, Supervision, Funding acquisition. **J.-L. Bobet:** Conceptualization, Validation, Resources, Writing - review & editing, Project administration, Supervision, Funding acquisition.

## Declaration of Competing Interest

The authors declare that they have no known competing financial interests or personal relationships that could have appeared to influence the work reported in this paper.

## Acknowledgements

S. Al Bacha acknowledges financial support from the Lebanese University and the AZM & SAADE Association. We thank Jean-Luc BRUNEEL for assistance with the Raman Microspectrometer and Prof. Neil Ayres for discussion.

## Appendix A. Supplementary data

Supplementary data to this article can be found online at https://doi.org/10.1016/j.elecom.2020.106813.

## References

[1] R. Prins, Hydrogen spillover. Facts and fiction, Chem. Rev. 112 (2012) 2714–2738, https://doi.org/10.1021/cr200346z.
[2] W. Curtis Conner, J.L. Falconer, Spillover in heterogeneous catalysis, Chem. Rev. 95 (1995) 759–788, https://doi.org/10.1021/cr00035a014.
[3] R. Prins, V.K. Palfi, M. Reiher, Hydrogen spillover to nonreducible supports, J. Phys. Chem. C 116 (2012) 14274–14283, https://doi.org/10.1021/jp212274y.
[4] M.W. Bartczak, J. Stawowska, Hydrogen atoms at the palladium surface, at the MgO surface and at the Pd-MgO metal-support boundary. Towards computer modelling of the spillover effect, Mater. Sci.- Poland 24 (2006) 421–432 https://dbc.wroc.pl/Content/1693/PDF/ms_vol24_2006_2_2.pdf#page=7.
[5] T. Ito, M. Kuramoto, M. Yoshioka, T. Tokuda, Active sites for hydrogen adsorption on magnesium oxide, J. Phys. Chem. 87 (1983) 4411–4416, https://doi.org/10.1021/j100245a019.
[6] A. Markmann, J.L. Gavartin, A.L. Shluger, Chemisorption of HCl to the MgO(001) surface: a DFT study, PCCP 8 (2006) 4359–4367, https://doi.org/10.1039/B608719A.
[7] G.X. Wu, J.Y. Zhang, Y.Q. Wu, Q. Li, K.C. Chou, X.H. Bao, Adsorption and dissociation of hydrogen on MgO surface: a first-principles study, J. Alloy. Compd. 480 (2009) 788–793, https://doi.org/10.1016/j.jallcom.2009.02.086.
[8] I.A. Pašti, M. Baljozović, N.V. Skorodumova, Adsorption of nonmetallic elements on defect-free MgO(001) surface – DFT study, Surf. Sci. 632 (2015) 39–49, https://doi.org/10.1016/j.susc.2014.09.012.
[9] H. Kobayashi, D.R. Salahub, T. Ito, Dissociative adsorption of hydrogen molecule on MgO surfaces studied by the density functional method, J. Phys. Chem. 98 (1994) 5487–5492, https://doi.org/10.1021/j100072a015.
[10] S. Coluccia, F. Boccuzzi, G. Ghiotti, C. Mirra, Evidence for heterolytic dissociation of $H_2$ on the surface of thermally activated MgO powders, Z. Phys. Chem. 121 (1980) 141–143, https://doi.org/10.1524/zpch.1980.121.1.141.
[11] N. Zobel, F. Behrendt, Activation energy for hydrogen abstraction from methane over Li-doped MgO: a density functional theory study, J. Chem. Phys. 125 (2006) 074715, , https://doi.org/10.1063/1.2227387.
[12] W. Karim, C. Spreafico, A. Kleibert, J. Gobrecht, J. VandeVondele, Y. Ekinci, J.A. van Bokhoven, Catalyst support effects on hydrogen spillover, Nature 541 (2017) 68–71, https://doi.org/10.1038/nature20782.
[13] M. Digne, P. Sautet, P. Raybaud, P. Euzen, H. Toulhoat, Use of DFT to achieve a rational understanding of acid–basic properties of γ-alumina surfaces, J. Catal. 226 (2004) 54–68, https://doi.org/10.1016/j.jcat.2004.04.020.
[14] A.L. Shluger, J.D. Gale, C.R.A. Catlow, Molecular properties of the magnesia surface, J. Phys. Chem. 96 (1992) 10389–10397, https://doi.org/10.1021/j100204a052.
[15] E.N. Gribov, S. Bertarione, D. Scarano, C. Lamberti, G. Spoto, A. Zecchina, Vibrational and thermodynamic properties of $H_2$ adsorbed on MgO in the 300–20 K interval, J. Phys. Chem. B 108 (2004) 16174–16186, https://doi.org/10.1021/jp0487410.
[16] I.E. Castelli, S.G. Soriga, I.C. Man, Effects of the cooperative interaction on the diffusion of hydrogen on MgO(100), J. Chem. Phys. 149 (2018) 034704, , https://doi.org/10.1063/1.5029329.
[17] E.A. Colbourn, W.C. Mackrodt, Theoretical aspects of $H_2$ and CO chemisorption on MgO surfaces, Surf. Sci. 117 (1982) 571–580, https://doi.org/10.1016/0039-6028(82)90539-8.
[18] S.A. Pope, M.F. Guest, I.H. Hillier, E.A. Colbourn, W.C. Mackrodt, J. Kendrick, Ab initio study of the symmetric reaction path of $H_2$ with a surface V center in magnesium oxide, Phys. Rev. B 28 (1983) 2191–2198, https://doi.org/10.1103/PhysRevB.28.2191.
[19] K. Hermansson, M. Baudin, B. Ensing, M. Alfredsson, M. Wojcik, A combined molecular dynamics–ab initio study of $H_2$ adsorption on ideal, relaxed, and temperature-reconstructed MgO(111) surfaces, J. Chem. Phys. 109 (1998) 7515–7521, https://doi.org/10.1063/1.477409.

[20] X.W. Zhou, F. El Gabaly, V. Stavila, M.D. Allendorf, Molecular dynamics simulations of hydrogen diffusion in aluminum, J. Phys. Chem. C 120 (2016) 7500–7509, https://doi.org/10.1021/acs.jpcc.6b01802.
[21] A.J. Du, S.C. Smith, X.D. Yao, G.Q. Lu, Hydrogen spillover mechanism on a Pd-doped Mg surface as revealed by ab initio density functional calculation, J. Am. Chem. Soc. 129 (2007) 10201–10204, https://doi.org/10.1021/ja0722776.
[22] C. Castellani, R.A. Lindtner, P. Hausbrandt, E. Tschegg, S.E. Stanzl-Tschegg, G. Zanoni, S. Beck, A.M. Weinberg, Bone-implant interface strength and osseointegration: biodegradable magnesium alloy versus standard titanium control, Acta Biomater. 7 (2011) 432–440, https://doi.org/10.1016/j.actbio.2010.08.020.
[23] M.K. Kulekci, Magnesium and its alloys applications in automotive industry, Int. J. Adv. Manuf. Technol. 39 (2008) 851–865, https://doi.org/10.1007/s00170-007-1279-2.
[24] B.L. Mordike, T. Ebert, Magnesium: properties — applications — potential, Mater. Sci. Eng., A 302 (2001) 37–45, https://doi.org/10.1016/S0921-5093(00)01351-4.
[25] A.A. Luo, Magnesium casting technology for structural applications, J. Magnesium Alloys 1 (2013) 2–22, https://doi.org/10.1016/j.jma.2013.02.002.
[26] T.R. Thomaz, C.R. Weber, T. Pelegrini, L.F.P. Dick, G. Knörnschild, The negative difference effect of magnesium and of the AZ91 alloy in chloride and stannate-containing solutions, Corros. Sci. 52 (2010) 2235–2243, https://doi.org/10.1016/j.corsci.2010.03.010.
[27] I.B. Singh, M. Singh, S. Das, A comparative corrosion behavior of Mg, AZ31 and AZ91 alloys in 3.5% NaCl solution, J. Magnesium Alloys 3 (2015) 142–148, https://doi.org/10.1016/j.jma.2015.02.004.
[28] C.C. Liu, S. Lu, Y.Y. Fu, H.P. Zhang, Flammability and the oxidation kinetics of the magnesium alloys AZ31, WE43, and ZE10, Corros. Sci. 100 (2015) 177–185, https://doi.org/10.1016/j.corsci.2015.07.020.
[29] S. Al Bacha, I. Aubert, O. Devos, M. Zakhour, M. Nakhl, J.L. Bobet, Corrosion of pure and milled $Mg_{17}Al_{12}$ in “model” seawater solution, Int. J. Hydrogen Energy 45 (2020) 15805–15813, https://doi.org/10.1016/j.ijhydene.2020.04.030.
[30] E. Koç, Corrosion behaviour of as cast β-$Mg_{17}Al_{12}$ phase in 3.5 wt% NaCl solution, Acta Phys. Polonica A 135 (2019) 881–883.
[31] H. Olijnyk, A.P. Jephcoat, Effect of pressure on Raman phonons in zirconium metal, Phys. Rev. B 56 (1997) 10751–10753, https://doi.org/10.1103/PhysRevB.56.10751.
[32] C. Ziparo, A. Giannasi, L. Ulivi, M. Zoppi, Raman spectroscopy study of molecular hydrogen solubility in water at high pressure, Int. J. Hydrogen Energy 36 (2011) 7951–7955, https://doi.org/10.1016/j.ijhydene.2011.01.178.
[33] G.L. Song, A. Atrens, Corrosion mechanisms of magnesium alloys, Adv. Eng. Mater. 1 (1999) 11–33, https://doi.org/10.1002/(sici)1527-2648(199909)1:1<11::Aid-adem11>3.0.Co;2-n.
[34] H. Ma, X.-Q. Chen, R.H. Li, S.L. Wang, J.H. Dong, W. Ke, First-principles modeling of anisotropic anodic dissolution of metals and alloys in corrosive environments, Acta Mater. 130 (2017) 137–146, https://doi.org/10.1016/j.actamat.2017.03.027.
[35] F.Y. Cao, G.-L. Song, A. Atrens, Corrosion and passivation of magnesium alloys, Corros. Sci. 111 (2016) 835–845, https://doi.org/10.1016/j.corsci.2016.05.041.
[36] S. Al Bacha, M. Zakhour, M. Nakhl, J.L. Bobet, Effect of ball milling in presence of additives (Graphite, $AlCl_3$, $MgCl_2$ and NaCl) on the hydrolysis performances of $Mg_{17}Al_{12}$, Int. J. Hydrogen Energy 45 (2020) 6102–6109, https://doi.org/10.1016/j.ijhydene.2019.12.162.
[37] J.F. Huang, G.-L. Song, A. Atrens, M. Dargusch, What activates the Mg surface—a comparison of Mg dissolution mechanisms, J. Mater. Sci. Technol. 57 (2020) 204–220, https://doi.org/10.1016/j.jmst.2020.03.060.